Supporting Information

Sensitive Microscale Thermophoresis Assay for Rapid Ochratoxin A Detection with Fluorescently Labeled Engineered Aptamer

Hao Yu,[1,2] Qiang Zhao[1,2,3 *]

1. State Key Laboratory of Environmental Chemistry and Ecotoxicology, Research Center for Eco-Environmental Sciences, Chinese Academy of Sciences, Beijing, 100085, China

2. University of Chinese Academy of Sciences, Beijing, 100049, China

3. School of Environment, Hangzhou Institute for Advanced Study, UCAS, Hangzhou 310024, China

[*] Corresponding Author, Email address: qiangzhao@rcees.ac.cn

Table S1 Sequences of aptamer probes

Name	Sequence
O29-3'FAM	5'-ATC GGG TGT GGG TGG CGT AAA GGG AGC AT-FAM-3'
O29-5'FAM	5'-FAM-ATC GGG TGT GGG TGG CGT AAA GGG AGC AT-3'
O31-3'FAM	5'-GAT CGG GTG TGG GTG GCG TAA AGG GAG CAT C-FAM-3'
O31-5'FAM	5'-FAM-GAT CGG GTG TGG GTG GCG TAA AGG GAG CAT C-3'
O32-3'FAM	5'-GAT CGG GTG TGG GTG GCG TAA AGG GAG CAT CG-FAM-3'
O32-5'FAM	5'-FAM-GAT CGG GTG TGG GTG GCG TAA AGG GAG CAT CG-3'
O33-3'FAM	5'-CGA TCG GGT GTG GGT GGC GTA AAG GGA GCA TCG-FAM-3'
O33-5'FAM	5'-FAM-CGA TCG GGT GTG GGT GGC GTA AAG GGA GCA TCG-3'
O36-3'FAM	5'-GAT CGG GTG TGG GTG GCG TAA AGG GAG CAT CGG ACA-FAM-3'
O36-5'FAM	5'-FAM-GAT CGG GTG TGG GTG GCG TAA AGG GAG CAT CGG ACA-3'

Table S2 Comparison of different aptamer probes in MST sensing OTA

Aptamer probes	Dynamic range (nM)	Detection limit (nM)	ΔF_{norm} (‰)	Signal responses	K_d (nM)
O29-3'FAM	-	-	-	-	-
O29-5'FAM	7.8-1000	7.8	45.0	decreasing	161.9 ± 31.0
O31-3'FAM	15.6-4000	15.6	313.5	decreasing	306.8 ± 21.8
O31-5'FAM	3.9-250	3.9	28.1	decreasing	16.9 ± 3.8
O32-3'FAM	2.0-1000	2.0	258.1	decreasing	24.5 ± 1.8
O32-5'FAM	2.0-4000	2.0	99.0	decreasing	63.6 ± 9.5
O33-3'FAM	1.0-500	1.0	27.2	decreasing	3.8 ± 2.1
O33-5'FAM	2.0-1000	2.0	17.4	increasing	16.0 ± 4.3
O36-3'FAM			NR		
O36-5'FAM	31.3-1000	31.3	11.5	decreasing	97.7 ± 15.4

Binding buffer was 20 mM Tris-HCl (pH 7.5), 20 mM KCl, and 20 mM $CaCl_2$. MST data were derived from F_{norm} (t=5 s).

O29-3'FAM showed two different normalized fluorescence signal trends among the OTA concentrations tested. O36-3'FAM did not show obvious changes in MST signals upon OTA binding.

K_d values were determined by MST analysis. NR means no response.

Table S3 **Effects of KCl concentration in binding buffer on the p**erformance of O32-3'FAM for MST sensing OTA

KCl concentration (mM)	K_d (nM)	ΔF_{norm} (‰)
0	113.1±21.9	16.2
1	40.9±3.0	152.6
5	12.8±1.7	291.8
10	12.0±2.0	318.0
20	11.6±1.6	340.8
50	13.8±1.9	227.7

Binding buffer contained 20 mM Tris-HCl (pH 8.5), 20 mM $CaCl_2$, 0.1% Tween 20, and various concentrations of KCl.

Table S4 **Effects of $CaCl_2$ concentration in binding buffer on the p**erformance of O32-3'FAM for MST sensing OTA

$CaCl_2$ concentration (mM)	K_d (nM)	ΔF_{norm} (‰)
0	NB	-
1	33.2±2.9	153.8
5	11.5±1.5	249.6
10	9.5±1.4	285.9
20	11.6±1.6	340.8
50	9.3±1.7	346.0

NB means no binding.

Binding buffer contained 20 mM Tris-HCl (pH 8.5), 20 mM KCl, 0.1% Tween 20, and various concentrations of $CaCl_2$.

Table S5 Comparison of some aptamer-based methods for OTA in terms of dynamic range and limit of detection (LOD).

Strategy	Dynamic range	LOD	Ref.
A catalytic aptasensor using nano-graphite-aptamer hybrid and DNase Ⅰ	20-400 nM	20 nM	40
A "signal-on" fluorescent method using FAM-labeled aptamer and single-walled carbon nanohorns	20-500 nM	17.2 nM	41
A regeneratable localized surface plasmon resonance aptasensor based on a gold nanorod	1.0 nM-10 μM	1.0 nM	42
Label-free aptasensor using SYBR Gold and exonuclease Ⅰ	20-500 nM	16.5 nM	43
Electrochemical aptasensor using strand-displacement polymerase reaction	30 pM-120 nM	5 pM	45
A fluorescent assay based on aptamer and complementary DNA	3.9-300 nM	3.9 nM	44
A label-free colorimetric aptasensor	0.1-82.8 nM	0.17 nM	46
Aptamer microscale thermophoresis assay	0.98 nM-1 μM	0.98 nM	This work

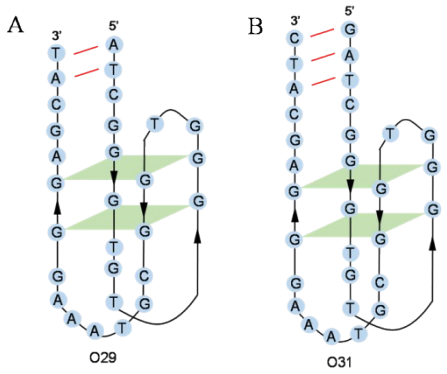

Figure S1. Diagram of secondary structures of aptamers O29 (A) and O31 (B).

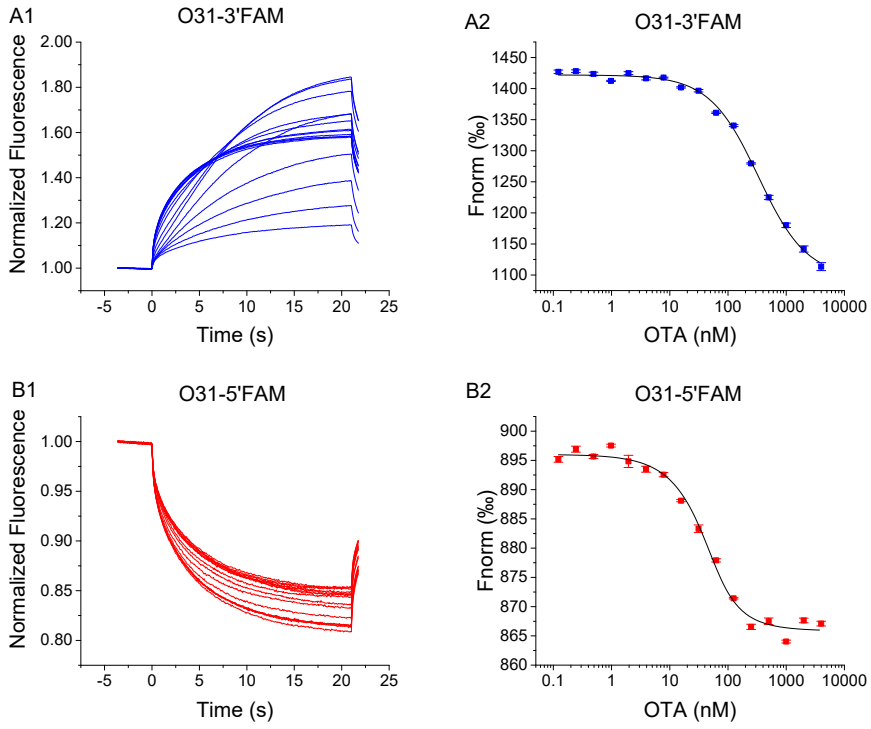

Figure S2. MST responses of O31-3'FAM (A1, A2) and O31-5'FAM (B1, B2) to OTA. MST time traces (A1, B1) and F_{norm} (t=5 s) signals (A2, B2) against concentrations of OTA were shown. Binding buffer was 20 mM Tris-HCl (pH 7.5), 20 mM KCl, and 20 mM $CaCl_2$.

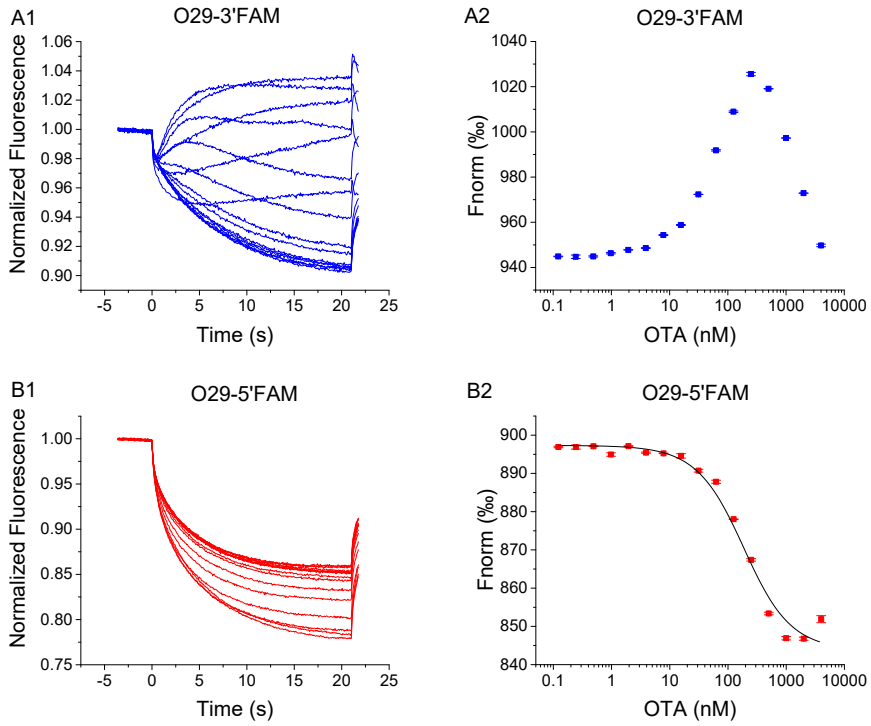

Figure S3. MST responses of O29-3'FAM (A1, A2) and O29-5'FAM (B1, B2) to OTA. MST time traces (A1, B1) and F_{norm} (t=5 s) signals (A2, B2) against concentrations of OTA were shown. Binding buffer was 20 mM Tris-HCl (pH 7.5), 20 mM KCl, and 20 mM $CaCl_2$.

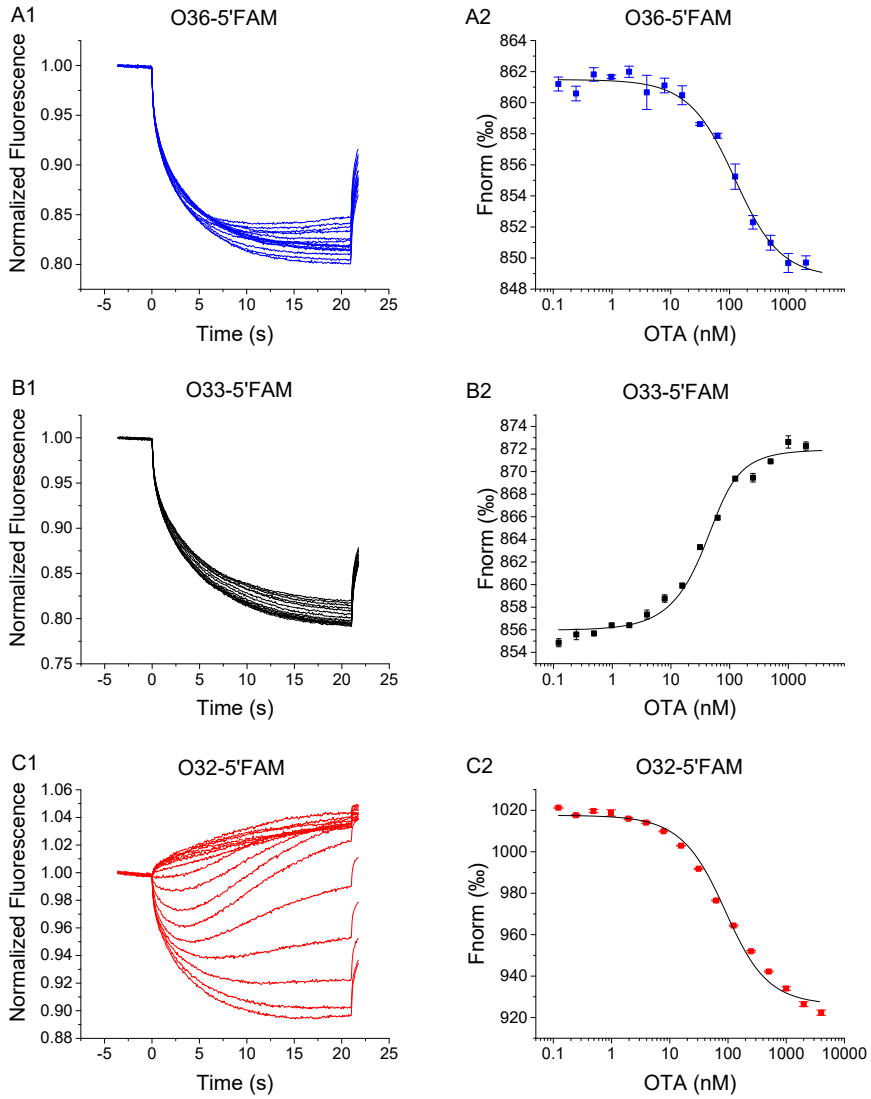

Figure S4. MST responses of O36-5'FAM (A1, A2), O33-5'FAM (B1, B2), and O32-5'FAM (C1, C2) to OTA. MST time traces (A1, B1, C1) and F_{norm} (t=5 s) signals (A2, B2, C2) against concentrations of OTA were shown. Binding buffer was 20 mM Tris-HCl (pH 7.5), 20 mM KCl, and 20 mM $CaCl_2$.

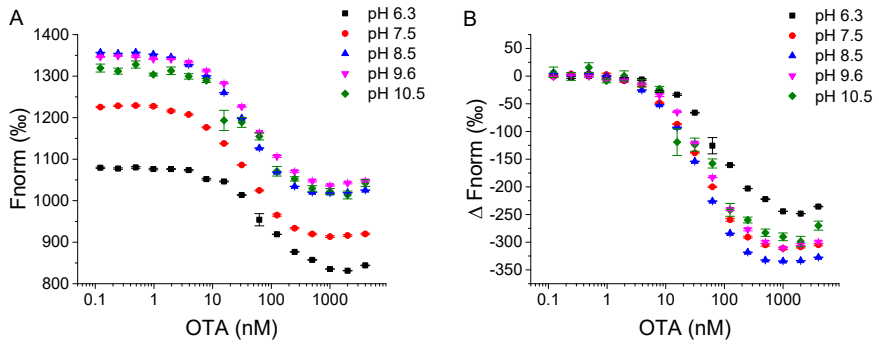

Figure S5. Effects of buffer pH on F_{norm} (t=5 s) (A) and ΔF_{norm} (B) of O32-3'FAM in response to different concentrations of OTA ranging from 0.12 nM to 4 μM. Binding buffer contained 20 mM Tris-HCl, 20 mM KCl, 20 mM $CaCl_2$, and 0.1% Tween 20.

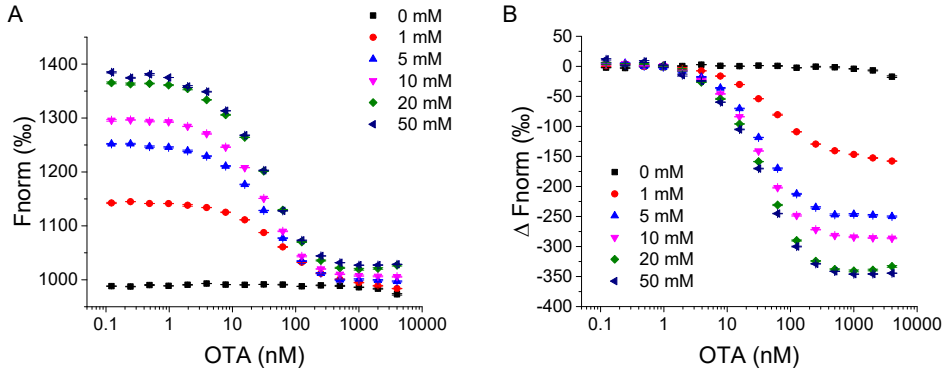

Figure S6. Effects of $CaCl_2$ concentration on F_{norm} (A) and ΔF_{norm} (B) of O32-3'FAM to different concentrations of OTA. Binding buffer contained 20 mM Tris-HCl (pH 8.5), 20 mM KCl, 0.1% Tween 20, and various concentrations of $CaCl_2$. Data from F_{norm} (t=5 s) were applied for analysis.

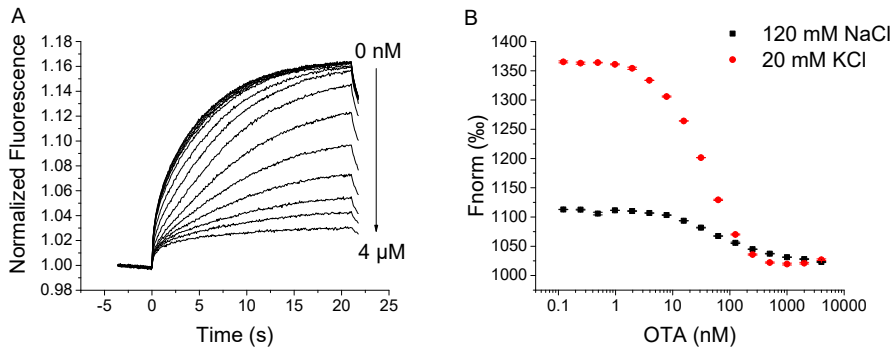

Figure S7. (A) MST fluorescence time curves of O32-3'FAM in response to varying concentrations of OTA in the buffer contained 20 mM Tris-HCl (pH 8.5), 20 mM $CaCl_2$, 120 mM NaCl, and 0.1% Tween 20. (B) Comparison of F_{norm} (t=5 s) responses of O32-3'FAM to OTA in different buffer conditions containing 120 mM NaCl or 20 mM KCl in the solution with 20 mM Tris-HCl (pH 8.5), 20 mM $CaCl_2$, and 0.1% Tween 20.

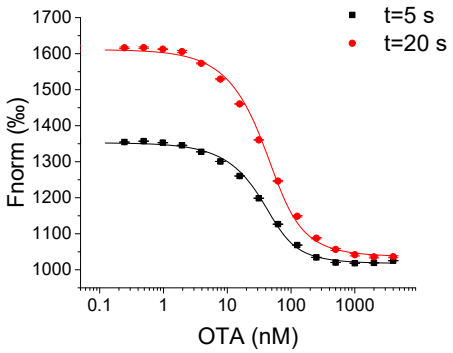

Figure S8. Comparison of F_{norm} to different concentrations of OTA at t=5 s and t=20 s by MST detection of OTA with O32-3'FAM.

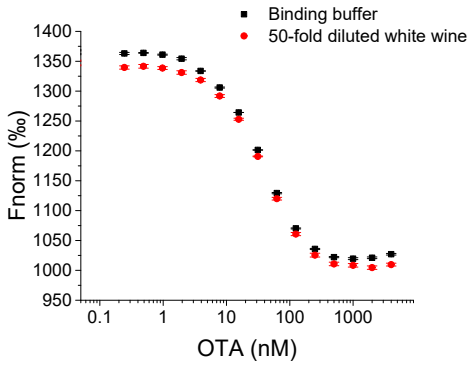

Figure S9. Detection of OTA in diluted white wine sample with O32-3'FAM.